HHS Public Access

Author manuscript

Dev Biol. Author manuscript; available in PMC 2016 December 01.

Published in final edited form as:

Dev Biol. 2016 October 15; 418(2): 248–257. doi:10.1016/j.ydbio.2016.08.003.

Small RNA *in situ* hybridization in *Caenorhabditis elegans*, combined with RNA-seq, identifies germline-enriched microRNAs☆

Tamara J. McEwen[#a,2], **Qiuming Yao**[#b], **Sijung Yun**[c], **Chin-Yung Lee**[d], and **Karen L. Bennett**[a,*,3]

[a] Molecular Microbiology and Immunology Department, University of Missouri School of Medicine, Columbia, MO 65212, USA

[b] Department of Computer Science, Bond Life Science Center, University of Missouri, Columbia, MO 65211, USA

[c] Yotta Biomed, LLC, 4835 Cordell Ave #1117, Bethesda, MD 20814, USA

[d] The Seydoux Laboratory, Molecular Biology and Genetics Department, Johns Hopkins School of Medicine, Baltimore, MD 21205, USA

[#] These authors contributed equally to this work.

Abstract

Over four hundred different microRNAs (miRNAs) have been identified in the genome of the model organism the nematode *Caenorhabditis elegans*. As the germline is dedicated to the preservation of each species, and almost half of all the cells in an adult nematode are germline, it is likely that regulatory miRNAs are important for germline development and maintenance. In *C. elegans* the *miR35* family has strong maternal effects, contributing to normal embryogenesis and to adult fecundity. To determine whether any particular miRNAs are greatly enriched in the *C. elegans* germline we used RNA-seq to compare the miRNA populations in several germline-defective strains of adult *C. elegans* worms, including *glp-4*(*germline proliferation-4*), *glh-1*(*germline helicase-1*) and *dcr-1*(*dicer-1*). Statistical analyses of RNA-seq comparisons identified 13 miRNAs that are germline-enriched, including seven members of the well-studied *miR35* family that were reduced as much as 1000-fold in TaqMan qRT PCR miRNA assays. Along with the *miR35s*, six others: *miR-56* (a member of the *miR51* family), *−70, −244, −260 , −788* and *−4813*, none of which previously considered as such, were also identified by RNA-seq as germline-enriched candidates. We went on to develop a successful miRNA *in situ* hybridization protocol for *C. elegans*, revealing *miR35*s specifically concentrate during oogenesis in the

☆**Note added in proof**: The Kohara group has also developed a *C. elegans* miRNA *in situ* hybridization protocol in a methods paper, Andachi and Kohara (2016) *RNA* July 22:1099-1106.

* Corresponding author. bennettk@missouri.edu (K.L. Bennett).
[2] Current address: Natural Sciences Division, Southwestern College, Winfield, KS 67156, USA.
[3] Professor Emerita, University of Missouri; Visiting Scientist, Seydoux Laboratory, USA.

Appendix A. Supplementary material

Supplementary data associated with this article can be found in the online version at http://dx.doi.org/10.1016/j.ydbio.2016.08.003.

pachytene region of the gonad, and persist throughout early embryogenesis, while in adult animals neither *let-7* nor *miR-228* has a germline-bias.

Keywords

glp-4; glh-1; dcr-1; *miR in situ* protocol; *miR35* family; let-7; miR-228

1. Introduction

Although microRNAs (miRNAs) were first described in *C. elegans* more than twenty years ago with the report of the *lin-4* small, temporal(st), non-coding(nc) RNA (Lee et al., 1993), the miRNA field exploded after the report of *let-7*, a second *C. elegans* miRNA affecting developmental timing, and one conserved in many other organisms, including humans (Pasquinelli et al., 2000). miRNAs, usually 21–22nts long, are endogenous to most plants and animals and are cleaved in the cytoplasm from hairpin precursor RNAs by the endo-ribonuclease Dicer. Mature miRNAs regulate their mRNA targets through antisense complementarity (often with mismatches), binding mRNAs in their UTRs (untranslated regions) or coding regions. miRNA binding causes post-transcriptional regulation of their targets, usually resulting in lower mRNA and/or protein levels.

For more than a decade many studies have implicated miRNAs as regulators of development and as markers of disease. While *lin-4* and *let-7*, and the *C. elegans* miRNA *lsy-6* (Johnston and Hobert, 2003), were each discovered by classical genetics and display visible mutant phenotypes, targeted deletion of over 80 individual miRNAs or closely linked miRNA families revealed only a few striking abnormalities. Exceptions include deletions in two families, the *miR51s* or *miR35s* that each result in embryonic lethality (Miska et al., 2007; Alvarez-Saavedra and Horvitz, 2010). The highly-conserved *miR51* family, consisting of *miRs-51-56* (*miR-100s* in humans), is likely the oldest group of animal miRNAs, found in annelids, nematodes, flies and humans. This family is critical for pharyngeal development in the *C. elegans* embryo (Shaw et al., 2010). The *miR35* family consists of eight miRNAs, each containing the same CACCGGC “seed” in their 5′ ends; *miR35s* are located in two clusters, with *miR-35-41* clustered together and *miR-42* 350 kb away. Microarray and northern analyses revealed the *miR35* family is strongly expressed in the oogenic germline (Miska et al., 2007), while additional studies revealed loss of this family results in embryonic death, male sterility and severe reductions in brood size (Alvarez-Saavedra and Horvitz, 2010; McJunkin and Ambros, 2014). Thus, the *C. elegans miR35s* are important both for embryonic development and to produce a normal adult germline.

In mammals, several recent studies have also considered roles for miRNAs in embryonic and germline development. In humans, the enhancement of somatic fates by the *let-7* miRNA family works in opposition to *miR-372*, which promotes human germ cell fates in embryonic stem cells (Tran et al., 2016), while in mice, sperm, as well as oocytes, transmit miRNAs and endo-siRNAs critical to the developing embryo (Yuan et al., 2016).

Despite elegant studies of miRNAs in *C. elegans* identifying miRNAs that are differentially expressed during development (Kato et al., 2009) or with ageing (Kato et al., 2011; Lucanic

et al., 2013), no studies targeting germline miRNAs have been reported. These studies were likely hindered by the inherent germline silencing of *C. elegans* transgenes, resulting in an inability of miRNA transgenes to express in the germline (Kelly et al., 1999; Martinez et al., 2008; Pierce et al., 2008; Shaw et al., 2010) and because *in situ* hybridizations for miRNAs in *C. elegans* had not yet been published, with the exception of *miR-57*, the most abundant miRNA in our RNA-seq studies, Supplemental Table S1, localizing to the posterior of a late-stage embryo (Zhao et al., 2010). Therefore, whether many miRNAs show a germline-bias was unknown.

Thus the goals of this study were to identify germline-enriched miRNA candidates and to develop methods to visualize *C. elegans* germline miRNAs by *in situ* hybridization. To do so, we carried out RNA-seq, followed by statistical analyses, utilizing the rather unique advantage available in *C. elegans* of multiple germline-minus and germline-defective mutant strains. With statistical comparisons using worms with and without germlines, 13 miRNAs were identified as germline-enriched. These include seven *miR35* family members, along with a single member of the *miR51* family, and five additional, individual miRNAs. To visualize the localization pattern of the *miR35* family, we also developed a successful *in situ* hybridization protocol and applied it to several other *C. elegans* miRNAs, including *miR-228* and *let-7*.

2. Materials and methods

2.1. Strains

Worm strains used for these studies include the following: wild type (N2 variety Bristol); VC178 [*glh-1*(*gk100*) I]; SS104 [*glp-4*(*bn2*) I]; and PD8753 [*dcr-1*(*ok247*) III/ghT2[bli-4(e937) let-?(q782) qIs48] (I;III)] (the ghT2, GFP-tagged chromosome, allows for selecting non-green homozygous *dcr-1* worms); and MT14119 [*miR-35-41*(*nDf50*) II] (This latter mutant carries a deletion of *miRs-35-41*, eliminating the polycistronic *miR-35-41* transcript (Alvarez-Saavedra and Horvitz, 2010)). All strains used in this study were maintained as described in (Brenner, 1974) and were grown at the optimal growth temperature of 20° unless otherwise noted. In this report strains will be referred to as follows: VC178 as *glh-1*; SS104 as *glp-4*; PD8753 as *dcr-1*, and MT14119 as *miR-35-41*.

2.2. Harvesting worms

Wild type (N2) and *glh-1* worms were placed at the first larval stage (L1) on NGM agar plates seeded with OP50 E. coli, cultured at 20° or 26° and harvested as young adults 1 day beyond the fourth larval stage (L4), when mature oocytes and embryos are first detected. N2s were harvested off approximately one hundred 15 × 100 mm plates and *glh-1* animals were harvested off approximately two hundred 15 × 60 mm plates by washing with M9 buffer (22 mM KH_2PO_4, 22 mM Na_2HPO_4, 86 mM NaCl). *glp-4* worms were cultured in liquid S media (10% S basal (0.1 M NaCl, 0.05 M potassium phosphate, 5 μg/ml cholesterol, 1 mM potassium citrate, 1 × trace metals solution [5 mM EDTA, 2.5 M $FeSO_4$, 1 mM $MnCl_2$, 1 mM $ZnSO_4$, 0.3 mM $MgSO_4$, 0.3 mM $CaCl_2$, 0.03 mM $MgSO_4$]) containing 7% χ1666 E. coli and incubated on an orbital shaker at 15° for ~6 days until the majority of worms in the culture were young adults full of embryos. The eggs in *glp-4* adults were

harvested by treatment with hypochlorite and grown until the adult stage at 26°. *glp-4* 26° adults were visually inspected for clear gonads, which indicates absence of a germline. All worms from a particular strain were combined and bacteria were cleared from the worms' cuticles and intestines by shaking in M9 for 45 min. This was followed by a wash in 1 × lysis buffer (50 mM HEPES pH 7.5, 1.0 mM EGTA, 3.0 mM $MgCl_2$, 100 mM KCl, 10% glycerol), with slurries of 1:1 volume of lysis buffer/worms stored in aliquots at −80°. Approximately 10,000 *dcr-1*(*ok427*) homozygous (non-green) worms were hand-picked and frozen in M9 and 50 × protease inhibitor (Complete™, mini, EDTA-free (Roche)). Multiple aliquots of *dcr-1* homozygous worms, collected over a period of time, were combined and RNA was isolated.

2.3. RNA isolation

Frozen worm lysate was thawed on ice and re-suspended in ~3 volumes of TRI-Reagent (Ambion, Inc). The TRI-Reagent/worm slurry was ground to a fine powder in liquid nitrogen and sonicated. After clearing insoluble debris, lysates were treated with 0.2 volume of chloroform, and the aqueous phase precipitated with equal volumes of isopropanol at −20°. RNA pellets were concentrated by centrifugation, and were stored in 10 mM Tris–HCl, pH7.5. RNA concentrations were determined with a Nanodrop ND1000 spectrophotometer; yields ranged from 2 to 5 μg/μL.

2.4. Small RNA enrichment

Small RNA fractions were enriched from *glp-4*, *glh-1*, N2, and *dcr-1* total RNA samples using the mirVana™ (Ambion, Inc) small RNA isolation protocol, with slight modifications as in (Gu et al., 2009). 5 μg aliquots were resolved on 2% agarose, MOPS-formaldehyde gels to visualize the RNAs prior to cDNA library construction and TaqMan® miRNA Assays.

2.5. Small RNA library construction and deep sequencing

The construction of cDNA libraries from small RNA templates and subsequent sequencing on the Illumina HiSeq-2000 was carried out by University of Missouri DNA Core Facility staff. Libraries were constructed from small RNAs from *glp-4* and *glh-1* mutant and N2 worms grown at 15°, 20° or 26°, and *dcr-1* mutants grown at 15°. For each strain and each tested temperature two cDNA libraries, each representing a unique biological replicate, were prepared with the Illumina® TruSeq™ Small RNA Sample Preparation kit as per the manufacturer's protocol. Each library was made from 2.5 μg of mir-Vana™-enriched small RNA and was individually identified with a short specific linker/adapter. The quality of construction was determined with an Agilent BioAnalyzer 2100 Chip. A plot illustrating this assay is shown in Supplemental Fig. S1. The cDNA libraries were sequenced using Illumina's HiSeq2000.

2.6. Bioinformatics

Sequencing data are available at NCBI in the Bioproject database with accession number PRJNA322183 (http://www.ncbi.nlm.nih.gov/bioproject/PRJNA322183). Data were generated by Illumina sequencing, with reads cleaned to remove low quality bases and

trimmed to remove the adaptors. All reads were aligned against the annotated, non-coding RNA transcripts downloaded from Wormbase ftp://ftp.wormbase.org/pub/wormbase/releases/WS242/species/c_elegans/PRJNA13758/c_elegans. PRJNA13758.WS242.ncrna_transcripts.fa.gz, which contains annotations for 223 miRNAs, 345 snoRNAs, 126 snRNA, 176 lincRNAs, 7980 ncRNAs, 15,365 piRNAs and other RNAs, including tRNAs, and rRNAs. The alignment from the above processed short reads to the non-coding transcripts was conducted using BWA, Burrows-Wheeler alignment (Li and Durbin, 2010). To obtain the counts for each miRNA, the HTSeq protocol (Anders et al., 2014) was applied to the mapping results, which are found in Supplemental Table S1.

Statistical tests comparing differential abundance levels between the miRNAs of various populations were carried out using DESeq2, a statistical analysis software available as an R/Bioconductor package (Love et al., 2014). DESeq2 software was used because it reports consistent results even for experiments with small number of replicates (Seyednasrollah et al., 2015). For our sequencing results DESeq2 provided much more conservative estimates of statistical significance than did the software package edgeR (Robinson et al., 2010). The adjusted p-value (q-value) of <0.05 was used as the cutoff for differential expression with statistical significance. q-values are adjusted p-values, used with the Benjamini-Hochberg procedure (Benjamini and Hochberg, 1995). http://www.stat.purdue.edu/~doerge/BIOINFORM.D/FALL06/Benjamini%20and%20Y%20FDR.pdf.

2.7. TaqMan® miRNA assays

qRT PCR was used to verify the RNAseq results for several candidates. Levels of *miR-38, −40, −228*, and *miR-244* were analyzed in *glp-4, glh-1, dcr-1* and wild type worms with TaqMan® MicroRNA Assays (Applied Biosystems). Quantitative PCR (qPCR) was performed in most cases with three independent biological samples, using triplicate technical replicates of each sample. Template cDNA specific for each miRNA was generated with the TaqMan® MicroRNA Reverse Transcription (RT) Kit as per the manufacturer's protocol. 10 ng of *glp-4* (15° and 26°), *glh-1* (26°), N2 (26° and 20°) or *dcr-1* (15°) mirVana™-enriched small RNA were used as the starting material for each 15 μL RT reaction. Products from each RT reaction were used as template for qPCR using TaqMan® Universal PCR Master Mix II (no UNG), with primers supplied by the manufacturer on a 7900HT Fast Real-Time PCR System (Applied Biosystems). Cycling conditions were: 95° for 10 min, and 40 cycles of 95° for 15 s and 60° for 1 min. Relative expression levels were determined according to (Pfaffl, 2001) and the delta-delta CT method (Schmittgen and Livak, 2008), using U18, a small nucleolar RNA transcript, as an endogenous control. Statistical analyses for these qPCRs were performed using T-tests, with the Relative Expression Software Tool (REST) 2009 (www.gene-quantification.de/rest.html).

2.8. in situ hybridizations

in situ hybridizations were carried out using modifications of the protocols reported by Seydoux and Fire (1994) for detecting messenger RNAs in *C. elegans* and by Pena et al. (2009) for localizing miRNAs in mouse tissue sections. Because the protocol is a new combination of others, it will be described in some detail here. *C. elegans* wild type and mutant worms were grown at 15°, 20° or 26 °C either to a young adult stage, when worms

first begin producing embryos (~1 day beyond the L4, fourth larval stage), or to a later adult stage, at 2–3 days beyond L4, when worms are fully gravid and the plates contain many embryos and newly-hatched larvae. Worms were placed in M9 buffer containing 1 mM levamisole, an anesthetic, and splayed onto poly-lysine-treated slides to provide access for the miRNA probes to the internal tissues. The slides were placed on dry ice to freeze-crack the adult tissues and embryos, using the light pressure of a coverslip. Slides were stored in 100% methanol at −20° for as little as 10 min, or for up to two weeks, before further fixation, hybridization and probe detection. After an additional 5 min in 100% methanol at RT, slides were rehydrated through an alcohol series of 90%, 70% and 50% methanol in TBS (150 mM NaCl, 50 mM Tris-HCl, pH7.5) for 1 min each, and were washed twice in TBS. All subsequent washes were in 1x TBS or TBS-T (TBS plus 0.1% Tween-20) for 5 min, all solutions were made with DEPC (diethylpyrocarbonate)-treated water and incubations were at RT unless noted otherwise. Throughout the fixation process TBS was used instead of PBS to avoid adding phosphate to the tissue, which would interfere with the EDC treatments to follow. The fixed tissue was then treated with 5 μg/ml, a mild dose of proteinase K (Roche) in 1x TBS for 15–20 min at RT, followed by exposure to 2 mg/ml glycine in TBS, and two TBS washes. An additional fixation for 20 min in 3.2% formaldehyde in a buffer of 80 mM HEPES, pH6.9, 16 mM $MgSO_4$, and 8 mM EGTA in TBS was followed by repeating the above glycine and wash steps. After the formaldehyde fixation, we followed the protocol of Pena et al., (2009) (Supplementary methods; Nat. Methods: doi.1038/nmeth.1294) using EDC (1-ethyl-3-(3-dimethylaminopropyl) carbodiimide), which significantly increases the levels of miRNAs remaining in the tissues by creating phosphoramidate linkages on the 5′ phosphates of the small RNAs. To first remove extraneous residual phosphates, slides were incubated twice, for 10 min, in 0.13 M 1-methylimidazole, 300 mM NaCl, pH8.0. Thereafter EDC was added to a concentration of 0.16 M into fresh 1-methylimidazole solution, placed on each slide and incubated for 2 h, followed by a third glycine treatment and two TBS washes. While the use of EDC was critical to our detection of a colorimetric signal, rather than storing EDC under argon, we purchased fresh aliquots of anhydrous EDC (Life Technologies) and brought this reagent up in the imidazole solution when needed for the *in situ* protocol. We also did not retain the harsh step of blocking all endogenous enzymatic activity with 0.1 M triethanolamine and 0.5% acetic anhydride that followed the EDC treatment (Pena et al., 2009).

After the EDC fixation, the slides were pre-hybridized for 2 h in a standard hybridization solution of 50% formamide, 5 × SSC, 5 × Denhardt's solution, 250 μg/ml yeast tRNA, 500 μg/ml herring DNA, 2% Blocking Reagent (Roche), and 0.1% CHAPS and 0.5% Tween-20 detergents. The miRNA probes tested were LNAs, locked nucleic acids, which are nuclease resistant; the LNAs we used were complementary to *miR-35, miR-38* and *miR-40, let-7* and *miR-228*. Controls included an LNA corresponding to the *C. elegans* pre-SL-1, the nuclear precursor of spliced leader-1, a small ncRNA involved in trans-splicing (Krause and Hirsh, 1987), as a positive control, and as a negative control, a scrambled LNA that does not correspond to any known *C. elegans* miRNA sequence; the LNAs were pre-labeled on both 5′ and 3′ ends with Digoxigenin (Exiqon). The MT14119 *miR-35–41* deletion strain was used as an additional negative control. Sequences of the LNA probes are found in Supplemental Table S2. Most probes were used for hybridization at a final concentration of

25 nM; however, when combined, the *miR-35, −38* and *−40* LNAs were each at 8 nM, while *miR-228* was at 50 nM. Probes were briefly heat denatured at 68° before added to the hybridization solution. Slides were covered with parafilm and hybridized in a humidified chamber for 13–16 h at 48 °C, a temperature > 20° below the T_m of any of the LNAs used (57° was also successful). After hybridization, 5x SSC was used to float off the parafilm and slides were washed twice for 30 min each in 1 × SSC; 50% formamide, 0.1% Tween-20 at 48°, then washed at RT in 0.2 × SSC for 15 min and finally in TBS-T. This was followed by blocking for endogenous peroxidase activity, with 3% hydrogen peroxide in TBS-T for 30 min, followed by three 1 min TBS-T washes.

To detect the hybridized probes, a antibody/amplification/antibody process was used. Slides were first blocked for 1 h at RT in 0.5% Blocking Reagent (Roche), with 10% heat-inactivated goat serum in TBS-T, followed by the addition of an anti-DIG-FAB peroxidase (POD, Roche) antibody diluted 1:500 in the above blocking solution and incubated for 1h at RT. Amplification of the peroxidase conjugate on the anti-DIG antibody was then achieved with the addition of the tyramide reagent that catalyzes deposits of dinityrophenyl (DNP) (TSA kit, PerkinElmer Renaissance® TSA™Plus DNP system NEL 747A). First, slides were washed 3 times in TNT buffer (0.1 M Tris-HCL, pH7.5, 0.15 M NaCl, 0.1% Tween-20) and then the tryamide solution was applied and incubated for 30 min, after which slides were washed 3 times in maleate buffer (0.09 M maleic acid, 0.175 M NaOH, 1 M NaCl, and 0.5% Tween-20, pH7.5). The DNP labels were subsequently detected by a second antibody reaction, with an anti-DNP antibody conjugated to Alkaline Phosphatase (AP) diluted 1:500 in the maleate buffer, supplemented with 10% blocking reagent (Roche); this reaction went for 40 min. Subsequent washes were twice in maleate buffer and four times in TMN buffer (0.1 M Tris-base, pH9.5, 0.05 M $MgCl_2$, 0.5 M NaCl, 0.05% Tween-20, and 2 mM tetramisole hybrochloride). These steps were as per manufacturer's directions.

The detection of signal followed using a colorimetric reaction with a BCIP/NBT solution (Roche Ready Mix tablets) that was allowed to proceed for 30 min, to allow an initial deposition of blue pigment, after which slides were incubated in KTBT (50 mM Tris-HCl, pH7.5, 150 mM NaCl, 10 mM KCl, with 1% Tween-20, a notably high detergent concentration) at 4° for 1–14 days and a second color reaction was carried out for an additional 30 min or more, until a strong signal was seen or the background became visible. This two-step color reaction, with KTBT buffer, was adapted from the GEISHA, chick protocols (Darnell et al., 2006) and made for a clearer, stronger signal. After completing the color reaction, slides were washed three times in a penultimate wash of 0.01 M Tris-HCL, pH7.5, 0.5 M NaCl. 5 mM EDTA, 0.05% Tween-20, followed by a 10 min fixation in a 4% aqueous paraformaldehyde solution, ending with a wash in water. Cover slips were applied using Vectashield mounting medium with DAPI (Vector Laboratories) and sealed with clear nail polish. Images were taken on a Zeiss Auxio Z1 microscope with SlideBox software and processed with Photoshop and Illustrator software. While the protocol used for these experiments was successful in repeated sets of experiments, using a single *miR35*- member probe was not effective. Future optimization of these in situ techniques for *C. elegans* may increase the sensitivity of miRNA detection.

3. Results

3.1. Comparing the small RNA transcriptomes of germline-defective C. elegans

To determine if any *C. elegans* miRNAs are enriched in the germline, we conducted deep sequencing on 14 cDNA libraries prepared from small RNA populations isolated from wild-type (N2) worms, grown at 20 °C and 26 °C, as well as from three germline-defective strains: *glp-4*(*bn2*) at 15 °C and 26 °C, *glh-1*(*gk100*) at 20 °C and 26 °C, and *dcr-1*(*ok247*) homozygous worms raised at 15 °C used as a control. Each library was constructed from a unique biological replicate. *glp-4*(*bn2*) is a mis-sense, partial loss of function mutation in *vars-2* (Rastogi et al., 2015), a gene coding for valine aminoacyl tRNA synthetase whose mRNA is highly enriched in the germline. *glp-4*(*bn2*) worms are fertile when grown at 15 °C, and are sterile when grown at the restrictive temperatures of 25–26 °C, with each hermaphrodite producing only ~12 germ cells compared to ~2000 in wild type (Beanan and Strome, 1992). *glh1*(*gk100*) is a non-null deletion allele in *glh-1*, a germline-specific RNA helicase component of P granules (Gruidl et al., 1996; Spike et al., 2008; Strome and Wood, 1983; Sheth et al., 2010). The truncated *glh-1*(*gk100*) product is expressed at ~10% of wild-type levels. *glh-1*(*gk100*) animals are fertile at 20 °C and 100% sterile at 26 °C, with under-proliferated germlines 1/5th-1/2 the normal size (Spike et al., 2008). The *glh-1* mutant was chosen for this study in part because GLH-1 is a binding partner of Dicer and therefore GLH-1 might have a role in processing miRNAs or other Dicer-dependent small RNAs (Beshore et al., 2011). The *dcr-1*(*ok247*) strain is a null mutation in the gene coding for the Dicer protein. *dcr-1*(*ok247*)hermaphrodites have fully developed germlines, but produce abnormal, endo-replicating germ cells (Ketting et al., 2001; Knight and Bass, 2001). The *dcr-1*(*ok247*) strain is balanced with a GFP-tagged chromosome and non-green, sterile, *dcr*-1homozygous adults were hand-picked to generate small RNAs for libraries and qRT-PCRs. All libraries were constructed using a 5′ ligation-dependent protocol that is specific for mono-phosphorylated species, which include micro-, piwi(pi)- and 26G RNAs; each library was individually tagged.

Deep sequencing of the multiple cDNA libraries generated from small RNA templates produced a total of 107,728,496 raw reads, 21,045,231 of which uniquely aligned to annotated, transcribed loci in the *C. elegans* genome. Of the uniquely aligned sequences, 5,064,689 reads mapped to 93 of the 223 annotated miRNA genes in WormBase.

ftp://ftp.wormbase.org/pub/wormbase/releases/WS242/species/c_elegans/PRJNA13758/c_elegans.PRJNA13758.WS242.ncrna_transcripts.fa.gz. In addition 62,364 reads mapped to 96 pre-miRNA genes, and 486,561 reads mapped to piRNAs. The reads mapping to other small RNAs are illustrated in Supplemental Fig. S2. Through use of the analysis pipeline of BWA and HTseq protocols (Li and Durbin, 2010; Anders et al., 2014), the raw mature miRNAs reads detected in all 14 libraries were determined; however, mature miRNA reads in the two *dcr-1* libraries were rare and are not included with the other 12 populations seen in Supplemental Table S1. Subsequently, the DESeq2 software program was used to examine the differentially-abundant miRNAs based directly on the read counts (Love et al., 2014). Both biological and technical variations were accommodated. We considered

miRNAs to be differentially expressed using the q-value of <0.05 as the cutoff for statistical significance.

3.2. Several miRNAs are significantly reduced when glp-4 worms lack a germline

Table 1A compares miRNA levels in *glp-4* mutants grown at 15° (fertile) versus 26° (sterile). Among the 93 miRNAs detected by our RNA-seq, we identified 21 miRNAs whose relative levels significantly decrease, and eight whose relative levels increase in sterile *glp-4* worms compared to fertile ones (Table 1A, Fig. 1A and Supplemental Table S3A). Because *glp-4* mutants raised at 26° consist mainly of somatic tissues, the former category likely correspond to miRNAs expressed preferentially in the germline, whereas the latter are likely to correspond to miRNAs expressed preferentially in the soma.

Since higher temperatures are known to adversely affect the fertility of wild type animals (Spike et al., 2008), we compared N2 worms grown at the optimal growth temperature of 20° to the more restrictive temperature, 26° and found no statistically significant differences among the 96 miRs detected by our RNAseq and the subsequent DESeq1 analysis, Supplemental Table S4.

We then went on to compare *glp-4* mutants grown at 26° to wild-type worms grown at 26° (Table 1B, and Fig. 1B). This comparison yielded 26 significantly mis-regulated mRNAs, including 17 down-regulated and nine up-regulated miRNAs. The gene overlap between the two *glp-4* comparisons (Table 1A-B and Fig. 1A-B) was 77% (13/17) for the down-regulated category and 56% (5/9) for the up-regulated category. Among the former, are 13 miRNAs including all seven *miR35* family members and six other unrelated *miRNAs, miR-56, −70, −244, −260, −788* and *−4813*, which we consider the “best candidates” for being germline-enriched. With regard to the down-regulated miRNAs that don't overlap in the two comparisons, we predict the four miRNAs only reduced in the comparison of *glp-4* 26° versus wild type animals grown at 26° may reflect specific effects of high temperature on the defective valine tRNA synthetase in the *glp-4*(*bn2*) animals, as three of these four miRNAs (*miR- 43,−61* and *1829.3*) are not reduced in wild type 26° animals, Supplemental Table S4.

One of the original aims of this research was to determine whether GLH-1, a constitutive P-granule component and a binding partner of Dicer (Beshore et al., 2011) affects germline miRNA levels. Therefore, we compared sterile *glh-1* mutants grown at 26° to fertile N2 worms grown at 26°. However, RNA-seq with sterile *glh-1* worms did not indicate all 13 of the germline-enriched miRNAs are statistically reduced, Table 1C. Four of the five reduced miRNAs, *miR-56, −244, −788* and *−4813*, are among the germline-enriched miRNAs identified in the *glp-4* analyses presented above, Table 1A-B. While these findings are consistent with sterile *glh-1* mutants having tiny germlines and fewer germ cells (Spike et al., 2008), seven other germline candidates were reduced, but not significantly, and two showed no reductions, Supplemental Table S3C. We also examined the levels of precursor miRNAs in *glh-1* mutants and did not find them obviously higher than those of N2 worms, in contrast to the accumulation of precursor miRNAs in *dcr-1* worms, Supplemental Table S5. Therefore, our RNA-seq analysis is inconclusive as to whether this *glh-1* strain affects the Dicer-dependent processing of all germline miRNAs. Perhaps too few replicates were tested or the limited response is due to this strongest *glh-1* mutant not being a null. The

GLH-1/DCR-1 germline complex might also function with the *C. elegans* 22Gs, endo-siRNAs that are critical in the germline for genome integrity and to repress selected protein coding sequences (Gu et al. 2009). In mice oocytes endo-siRNAs are essential for meiotic maturation (Stein et al. 2015). While the 22Gs are, like miRNAs, Dicer-dependent, they are not mono-phosphorylated, and therefore are not in our libraries. Thus, the basis of the DCR-1/GLH-1 relationship (Beshore et al., 2011) remains to be determined.

3.3. Verification of the RNA-seq results using qRT-PCR

To independently verify some of the changes observed by RNA-seq, we carried out qRT-PCR for four miRNAs, three predicted to be preferentially expressed in the germline based on the RNA-seq data and one, *miR-228*, predicted to be expressed both in the soma (Pierce et al., 2008) and germline (Table 1A–C). As many as nine replicate TaqMan qRT-PCRs compared: (i). *glp-4* 26° levels against *glp-4* 15° worms, (ii). *glh-1* worms against N2s, both grown at 26°, and as a control (iii). *dcr-1*, raised at 15°, vs. fertile N2 adults grown at 20°, Fig. 1C and Table 2. Quantification of the qRT-PCR results for *glp-4* confirmed the RNA-seq results, panel 1. We observed the most dramatic changes for the two *miR35* family members tested, with reductions as high as 1000-fold for *miR-35* in *glp-4* sterile mutants, Fig. 1C, panel 1 and Table 2. When fertile N2 worms were tested against sterile *glh-1* animals, all four probes were significantly reduced in the qRT PCR assays, Fig. 1C, panel 2 and Table 2. Perhaps unexpectedly, both *miR-38* and *−40*, which were not significantly reduced in the DESeq2 analysis of sterile *glh-1* worms, Supplemental Table S3C, were significantly reduced with the increased numbers of biological and technical replicates used for qRT PCR, Fig. 1C, panel 2, and Table 2, further supporting the germline-enrichment of the *miR35s*. As expected, the *dcr-1* RNA showed significant reductions for all miRNAs tested, Fig. 1C, panel 3 and Table 2. However, the markedly greater fold changes for the *miR35* probes in the germcell-less *glp-4* animals than seen for *dcr-1* null mutants might be unexpected, Table 2. We note that *dcr-1* animals have large, albeit abnormal, germlines, and therefore, could retain higher levels of stable, maternal miRNAs than the germline-minus *glp-4* animals. Therefore, we propose this result is likely due to the perdurance of maternal miRNAs in the *dcr-1* mutant, a suggestion also made by Drake et al. (2014) when studying Dicer-1 and observing “only modest differences in bulk miRNA levels between WT and *dcr-1*(*0*) animals”.

3.4. in situs indicate miR35s are highly enriched in the adult germline

To visualize the localization of miRNAs in *C. elegans*, we developed an *in situ* hybridization protocol for miRNAs based on techniques reported for chick and mouse miRNAs (Darnell et al., 2006; Pena et al., 2009) as detailed in Section 2.

Hybridizations were carried out on adult *C. elegans* worms that had been splayed open to release their gonads, partially removing the germline (red arrows), as well as the intestinal tissue (black arrows), away from the body wall cavity, Fig. 2. A cartoon of the two symmetric gonad arms as they appear in an intact adult worm illustrates the normal developing germline, Fig. 2A. In Fig. 2B, strong hybridization is seen in the meiotic pachytene region of the gonad where oogenic and maternal RNAs are abundantly transcribed (red arrow), when a combined LNA probe complementary to the mature miRNAs

corresponding to *miR-35, −38* and *−40* was used. In Fig. 2C, the *miR35s* are also detected with the combined *miR35* probe in the oocytes and embryos (white arrow) of this older adult. A five-fold extension of the color reaction time using two probes, *miR-38* and *−40*, revealed staining throughout both completely-removed gonad arms, beginning in the distal region (red arrow) in this young adult animal, Fig. 2D. Even with this extended exposure, no signal was detected in the adjacent, isolated intestinal tissue (or in other somatic tissues), Fig. 2D, despite previous studies with a *miR35* promoter-driven GFP transgene indicating GFP expression in the vulva, several anterior neurons and the rectum (Martinez et al., 2008). This difference in findings may reflect a lack of sensitivity of the current *in situ* protocol or a failure to penetrate the hard cuticle of the adult body wall with the relatively mild treatments used for fixation, Section 2. A DAPI image of Fig. 2D is seen in Fig. 2E. As negative controls, the mutant strain MT14119 *miR-35-41*(*nDf50*) was tested, Fig. 2F, with only background hybridization detected with the combined *miR35* probe, while a scrambled LNA also produced no signal, Fig. 2G. Both negative controls were carried out for ~1 h, the same exposure used for Figs. 2B-C, and 2H-I, and for the positive SL-1 probe, which revealed concentrated nuclear staining for the SL-1 precursor, Supplemental Fig. S3, in contrast to the uniform, cytoplasmic staining of the mature miRNAs seen here, Fig. 2B-D and H-I. In addition, a *let-7* LNA probe produced no signal in N2 adult tissues or wild type embryos (not shown), an expected result based on the rarity of *let-7* in our libraries, Supplemental Table S1. However, surprisingly, we did detect *let-7* hybridization in the abnormal embryos of the *miR-35-41* deletion strain, Fig. 2H; this staining appears to reveal inappropriate embryonic expression of *let-7* when the *miR35s* are missing. This could relate to findings in (Akay et al., 2013) that both *miR35* and *let7* families genetically interact with GLD-1, a well-studied RNA binding protein. While Brenner and Schedl (2016) present convincing evidence that GLD-1 is not a target of the *miR35s*, we suggest GLD-1 may indirectly regulate these two miRNA families and that when one miRNA family is missing, the other increases in expression. In Fig. 2I, in contrast to the exclusive germline location of the *miR35s* seen by *in situ* hybridizations in Fig. 2B-D, we detected strong signals in both the intestine and in the distal germline with a *miR-228* probe. As the *C. elegans miR-228* (*miR-183* in mammals) was previously seen in multiple somatic tissues by GFP expression (Pierce et al., 2008) and based on our RNA-seq and qRT-PCR results, this dual localization was not unexpected. In summary, these *in situ* hybridizations are consistent with our RNA-seq results, Table 1A-B, and provide the first visualization of the *miR35* microRNAs as highly enriched the adult germline, concentrating in the pachytene region and in maturing oocytes; they also reveal expected localizations for *miR-228* and both expected and unexpected patterns for *let-7*.

4. Discussion

We have compared the miRNA transcriptomes of wild-type and germline-defective worms and have identified 13 miRNAs that are preferentially expressed in the germline. These include seven of the eight members of the *miR35* family, which appear highly enriched in germ cells. In using our newly developed *in situ* hybridization protocol to detect miRNAs in *C. elegans* tissues, the *miR-35-41* miRNAs appear exclusive to the germline of adult hermaphrodites. These miRNAs are first detected during oogenesis and accumulate at high

levels in oocytes and early embryos. Our findings are consistent with the genetic findings of (Alvarez-Saavedra and Horvitz, 2010) who determined that deletion of seven of the eight *miR35* family members causes temperature-sensitive, maternal-effect and zygotic lethality, resulting in embryonic or L1 larval arrest, while loss of all members is lethal at all temperatures.

Since many miRNAs have been individually deleted (Miska, et al., 2007), the phenotypes resulting from the loss of some of the germline miRNAs identified here have already have been reported. As described above, deletion of all *miR35* family members results in embryonic lethality; however adding back maternal expression of the *miR35–41* gene cluster or of each individual *miR35* member, results in normal embryonic development (Alvarez-Saavedra and Horvitz, 2010), implying redundancy of the *miR35*s and a vital role for this family in embryonic development. In addition, McJunkin and Ambros (2014) have demonstrated that maternal, along with zygotic, *miR35s* act early in development to insure maximal fertility of the adult progeny, while Brenner and Schedl (2016) quantified the marked reduction in proliferation in the *C. elegans* germline with loss of all *miR35* family members. In the *miR51* family, *miR-56* is the only member we identified as germline-enriched. Deletion of all six *miR51* genes results in dead embryos, with any individual *miR51* member able to rescue the embryonic lethality (Shaw et al., 2010); however, a specific role for *miR-56* in the adult germline had not been reported. There are no deletions reported for *miR-788* and *−4813*; these two more recently-discovered miRNAs were not a part of the large deletion study by the Horvitz group (Miska et al., 2007). There are individual deletions of *miR-70, −244* and *−260*, which revealed no gross abnormalities, supporting the conclusions of others, including (Miska et al., 2007; Alvarez-Saavedra and Horvitz, 2010) that the normal regulatory functions of most individual miRNAs are likely subtle. And while studies in mammals have demonstrated that most germline miRNAs lack function in mouse oocytes or during early embryonic development (Suh et al., 2010), similar studies are incomplete in *C. elegans*. In addition, recent findings in mammals suggest that individual miRNAs have decisive roles in promoting germline development, as seen for human *miR-372* (Tran et al., 2016). Therefore, in addition to the established maternal contributions of the *miR35* and *miR51* families, we predict additional individual and opposing *C. elegans* miRNA teams also contribute to germline development.

Nine of the 13 germline miRNA candidates identified here are among the 50+ miRNAs that change in abundance as hermaphrodites age and cease reproduction (Kato et al., 2011; Lucanic et al., 2013). In particular, six members of the *miR35* family dramatically increase in abundance in aged, post-reproductive worms, while *miR-70, −244*, and *−788* decrease. The Lucanic studies also used the germline-minus strain *glp-1*(*e2141*) to further verify the age-dependent differences in levels of *miR-35, −37* and *−244*; however, whether these germline miRNAs play a role in aging has not yet been established. Interestingly, only one of the germline miRNAs, *miR-70*, was reported as a miRNA that is abundant in embryos and increases in abundance during larval development, while *miR-35, −37* and *−40* decrease dramatically following embryogenesis and remain at low levels until adulthood (Kato et al., 2009). Perhaps *miR-70* is involved in the establishment of the germline that begins in embryos and progresses in larvae, while the other 12 germline miRNAs function as maternal (or paternal) transcripts critical to embryogenesis, or in maintenance of the adult germline.

In summary, RNA-seq and the differential statistical comparisons in this report have identified 13 miRNAs that are preferentially expressed in the germline of adult hermaphrodites. These studies have further parsed the relationships of individual miRNAs in the *miR-35* and *−51* families and have taken the *C. elegans* miRNA field beyond these two very interesting families, with striking embryonic phenotypes and germline connections, to reveal five additional, germline-enriched miRNAs. We anticipate future studies will reveal these five newly-identified miRNAs also play important roles in development, either individually or in concert.

Supplementary Material

Refer to Web version on PubMed Central for supplementary material.

Acknowledgments

We thank Bill Spollen, bioinformatics specialist at MU, who advised QY and TJM in their bioinformatics analyses and Dr. Darryl Conte, UMass, for technical advice regarding small RNA isolation. KLB thanks Geraldine Seydoux and Depika Calidas for critical manuscript review and the Seydoux lab members, especially Alex Paix for *in situ* advice and Dominique Rasoloson for technical help, and Sally Moody and her lab at George Washington U, who also hosted KLB. This work was supported by NSF funding IOS-0819712 (KLB), a University of Missouri Life Sciences Fellowship (TJM), and NIH grant NICHD90042240 to G. Seydoux for partial support of KLB.

References

Akay A, Craig A, Lehrbach N, Larance M, Pourkarimi E, Wright JE, Lamond A, Miska E, Gartner A. RNA-binding protein GLD-1/quaking genetically interacts with the mir-35 and the let-7 miRNA pathways in *Caenorhabditis elegans*. Open Biol. 2013; 3:130151. [PubMed: 24258276]

Alvarez-Saavedra E, Horvitz HR. 'Many families of *C. elegans* microRNAs are not essential for development or viability'. Curr. Biol. 2010; 20:367–373. [PubMed: 20096582]

Anders, S.; Pyl, PT.; Huber, W. HTSeq, a Python framework to work with high-throughput sequencing data.. Bioinformatics. 2014. http://dx.doi.org/10.1096/bioinformatics/btu638. epub 2014Sept 23

Beanan MJ, Strome S. Characterization of a germ-line proliferation mutation in *C. elegans*. Development. 1992; 116(3):755–766. [PubMed: 1289064]

Benjamini Y, Hochberg Y. Controlling the false discovery rate: a practical and powerful approach to multiple testing. J. R. Stat. Soc. Ser. B. 1995; 57(1):289–300.

Beshore EL, McEwen TJ, Jud MC, Marshall JK, Schisa JA, Bennett KL. '*C. elegans* Dicer interacts with the P-granule component GLH-1 and both regulate germline RNPs'. Dev. Biol. 2011; 350(2): 370–381. [PubMed: 21146518]

Brenner JL, Schedl T. Germline stem cell determination entails regional control of cell fate regulator GLD-1 in *Caenorhabditis elegans*. Genetics. 2016; 202:1085–1103. [PubMed: 26757772]

Brenner S. The genetics of *Caenorhabditis elegans*. Genetics. 1974; 77(1):71–94. [PubMed: 4366476]

Darnell DK, Kaur S, Stanslaw S, Konieczka JH, Yatskievych TA, Antin PB. 'MicroRNA expression during chick embryo development'. Dev. Dyn. 2006; 235(11):3156–3165. [PubMed: 17013880]

Drake M, Furuta T, Suen KM, Gonzaalez G, Liu B, Kalia A, Ladbury JE, Fire A,Z, Skeath JB, Arur S. A requirement for ERK-dependent Dicer phosphorylation in coordinating oocyte-to-embryo transition in *C. elegans*. Dev. Cell. 2014; 31:614–628. [PubMed: 25490268]

Gruidl ME, Smith PA, Kuznicki KA, McCrone JS, Kirchner J, Roussell DJ, Strome S, Bennett KL. 'Multiple potential germline helicases are components of the germline-line specific P granules of Caenorhabditis'. Proc. Natl. Acad. Sci. USA. 1996; 93(24):13837–13842. [PubMed: 8943022]

Gu W, Shirayama M, Conte D Jr. Vasale J, Batista PJ, Claycomb JM, Moresco JJ, Youngman EM, Keys J, Stoltz MJ, Chen CC, Chaves DA, Duan S, Kasschau KD, Fahlgren N, Yates JR 3rd, Mirani S, Carrington JC, Mello CC. Distinct Argonaute-mediated 22G-RNA pathways direct genome surveillance in the *C. elegans* germline. Mol. Cell. 2009; 36(2):231–244. [PubMed: 19800275]

Johnston RJ, Hobert O. 'A microRNA controlling left/right neuronal asymmetry in *C. elegans*'. Nature. 2003; 426(6968):845–849. [PubMed: 14685240]

Kato M, de Lencastre A, Pincus Z, Slack FJ. 'Dynamic expression of small non-coding RNAs, including novel microRNAs and piRNAs/21U-RNAs, during *Caenorhabditis elegans* development'. Genome Biol. 2009; 10(5):R54. [PubMed: 19460142]

Kato M, Chen X, Inukai S, Zhao H, Slack FJ. 'Age-associated changes in expression of small, noncoding RNAs, including microRNAs, in *C. elegans*'. RNA. 2011; 17:1804–1820. [PubMed: 21810936]

Kelly WG, Xu S, Montgomery MK, Fire A. 'Distinct requirements for somatic and germline expression of a generally expressed *Caernorhabditis elegans* gene'. Genetics. 1999; 146(1):227–238.

Ketting RF, Fischer SE, Bernstein E, Sijen T, Hannon GJ, Plasterk RH. 'Dicer functions in RNA interference and in synthesis of small RNA involved in developmental timing in *C. elegans*. Genes Dev. 2001; 15(20):265–269.

Knight SW, Bass BL. 'A role for the RNase III enzyme DCR-1 in RNA interference and germ line development in *Caenorhabditis elegans*'. Science. 2001; 293(5538):2269–2271. [PubMed: 11486053]

Krause M, Hirsh D. 'A trans-spliced leader sequence on actin mRNA in *C. elegans*'. Cell. 1987; 49(6): 753–761. [PubMed: 3581169]

Lee RC, Feinbaum RL, Ambros V. 'The *C. elegans* heterochronic gene lin-4 encodes small RNAs with antisense complementarity to LIN-14'. Cell. 1993; 75:843–854. [PubMed: 8252621]

Li H, Durbin R. Fast and accurate long-read alignment with Burrows-Wheller transform. Bioinformatics. 2010; 26(5):589–595. http://dx.doi.org/10.1093/bioinformatics/btp698/ Epub2010 Jan15. [PubMed: 20080505]

Love ML, Huber W, Anders S. 'Moderate estimate of fold change and dispersion for RNA-seq data with DESeq2'. Genome Biol. 2014; 15(12):550–571. [PubMed: 25516281]

Lucanic M, Graham J, Scott G, Bhaumik D, Benz CC, Hubbard A, Lithgow GJ, Melov S. 'Age-related micro-RNA abundance in individual *C. elegans*'. Aging. 2013; 5(6):394–411. [PubMed: 23793570]

Martinez NJ, Ow MC, Reece-Hoyes JS, Barrasa MI, Ambros VR, Walhout AJM. 'Genome-scale spatiotemporal analysis of *Caenorhabditis elegans* microRNA promoter activity'. GenomeRes. 2008; 18:2005–2015.

McJunkin K, Ambros V. The embryonic *miR-35* family of microRNAs promotes multiple aspects of fecundity in *Caenorhabditis elegans*. G3. 2014; 4:1747–1754. [PubMed: 25053708]

Miska EA, Alvarez-Saavedra E, Abbott AL, Lau NC, Hellman AB, McGonagle SM, Bartel DP, Ambros VR, Horvitz HR. 'Most *Caenorhabditis elegans* microRNAs are individually not essential for development or viability'. PLoS Genet. 2007; 3:e215. [PubMed: 18085825]

Pasquinelli AE, Reinhart BJ, Slack F, Martindale MQ, Kuroda MI, Maller B, Hayward DC, Ball EE, Degnan B, Müller P, Spring J, Srinivasan A, Fishman M, Finnerty J, Corbo J, Levine M, Leahy P, Davidson E, Ruvkun G. 'Conservation of the sequence and temporal expression of *let-7* heterochronic regulatory RNA'. Nature. 2000; 408:86–89. [PubMed: 11081512]

Pena JTG, Sohn-Lee C, Rouhanifard SH, Ludwig J, Hafner M, Milhailovic A, Lim C, Holoch D, Berninger P, Zavolan M, Tuschl T. 'miRNA in situ hybridization in formaldehyde and EDC-fixed tissues. Nat. Methods. 2009; 6(2):139–141. [PubMed: 19137005]

Pfaffl MW. 'A new mathematical model for relative quantification in real-time RT-PCR. Nucleic Acids Res. 2001; 29(9):e45. [PubMed: 11328886]

Pierce ML, Weston MD, Fritzsch B, Gabel HW, Ruvkun G, Soukup GA. 'MicroRNA-183 family conservation and ciliated neurosensory organ expression. Evol. Dev. 2008; 10(11):106–113. [PubMed: 18184361]

Rastogi S, Borgo B, Pazdernik N, Fox P, Mardis ER, Kohara Y, Havranek J, Schedl T. *Caenorhabditis elegans* glp-4 encodes a valyl aminoacyl tRNA synthetase. G3. 2015; 5(12):719–728. http://dx.doi.org/10.1534/g3.115.021899. [PubMed: 25740935]

Robinson MD, McCarthy DJN, Smyth GR. 'edge R: a Bioconductor package for differential expression analysis of digital gene expression data. Bioinformatics. 2010; 26(1):139–140. doi: 10.1093 bioinformatics/btp616 epub 2009 Nov11. [PubMed: 19910308]

Schmittgen TD, Livak KJ. 'Analyzing real-time PCR data by the comparative C(T) method'. Nat. Protoc. 2008; 3(6):1101–1108. [PubMed: 18546601]

Seydoux G, Fire A. Whole mount in situ hybridization for the detection of RNA in *Caenorhabditis elegans* embryos. Development. 1994; 120(10):2823–2834. [PubMed: 7607073]

Seyednasrollah F, Larho A, Elo LL. 'Comparison of software packages for detecting differential expression in RNA-seq stuies'. Brief. Bioinform. 2015; 16(1):59–70. http://dx.doi.org/10.1093/bib/bbt086. [PubMed: 24300110]

Shaw WR, Armissen J, Lehrbach NJ, Miska EA. 'The conserved miR-51 microRNA family is redundantly required for embryonic development and pharynx attachment in C. elegans'. Genetics. 2010; 185(3):897–905. [PubMed: 20421599]

Sheth U, Pitt J, Dennis S, Priess JR. 'Perinuclear P granules are the principal sites of mRNA export in adult *C. elegans* germ cells'. Development. 2010; 137(8):1300–1314.

Smith PA, Leung-Chiu WM, Montgomery R, Osborn A, Kuznicki KA, Gressman-Coberly E, Mutapcic L, Bennett KL. The GLH proteins, *Caenorhabditis elegans* P granule components, associate with CSN-5 and KGB-1, proteins necessary for fertility, and with ZYX-1, a predicted cytoskeletal protein'. Dev. Biol. 2002; 251:333–347. [PubMed: 12435362]

Spike C, Meyer N, Racen E, Orsborn A, Kirchner J, Kuznicki K, Yee C, Bennett KL, Strome S. 'Genetic analysis of the *Caenorhabditis elegans* GLH family of P-granule proteins'. Genetics. 2008; 178(4):1973–1987. [PubMed: 18430929]

Stein P, Rozhkov NV, Li F, Cardenas FL, Davydenko O, Vandiver LE, Gregory BD, Hannon GJ, Schultz RM. Essential role for endogenous siRNAs during meiosis in mouse oocytes'. PLoS Genet. 2015; 11(4):e1005129. http://dx.doi.org/10.1371/journal.pgen.1005013. [PubMed: 25860788]

Strome S, Wood WB. Generation of asymmetry and segregation of germline granules in early *C. elegans*. Cell. 1983; 35:15–25. [PubMed: 6684994]

Suh N, Baehner L, Moltzahn R, Melton C, Shenoy A, et al. MicroRNA function is globally suppressed in mouse oocytes and early embryos. Curr. Biol. 2010; 20:271–277. http://dx.doi.org/10.1016/cub.2009.12.044. pmid:201116247. [PubMed: 20116247]

Tran, ND.; Kissner, M.; Subramanyam, D.; Parchem, RJ.; Laird, DJ.; Blelloch, RH. A miR-372/let-7 axis regulates human germ versus somatic cell fates.. Stem Cells. 2016. http://dx.doi.org/10.1002/stem.2378 (Epub ahead of print)

Yuan S, Schuster A, Tang C, Yu T, Ortongero N, Bao J, Zheng H, Yan V. 'Sperm-borne miRNAs and *endo*-siRNAs are important for fertilization and preimplantation embryonic development'. Development. 2016; 143(4):636–647.

Zhao Z, Boyle T, Liu Z, Murray JI, Wood WB, Waterston RH. 'A negative regulatory loop between microRNA and Hox gene controls posterior identities in Caenorhabditis elegans'. PLoS Genet. 2010; 6(9):e1001089. [PubMed: 20824072]

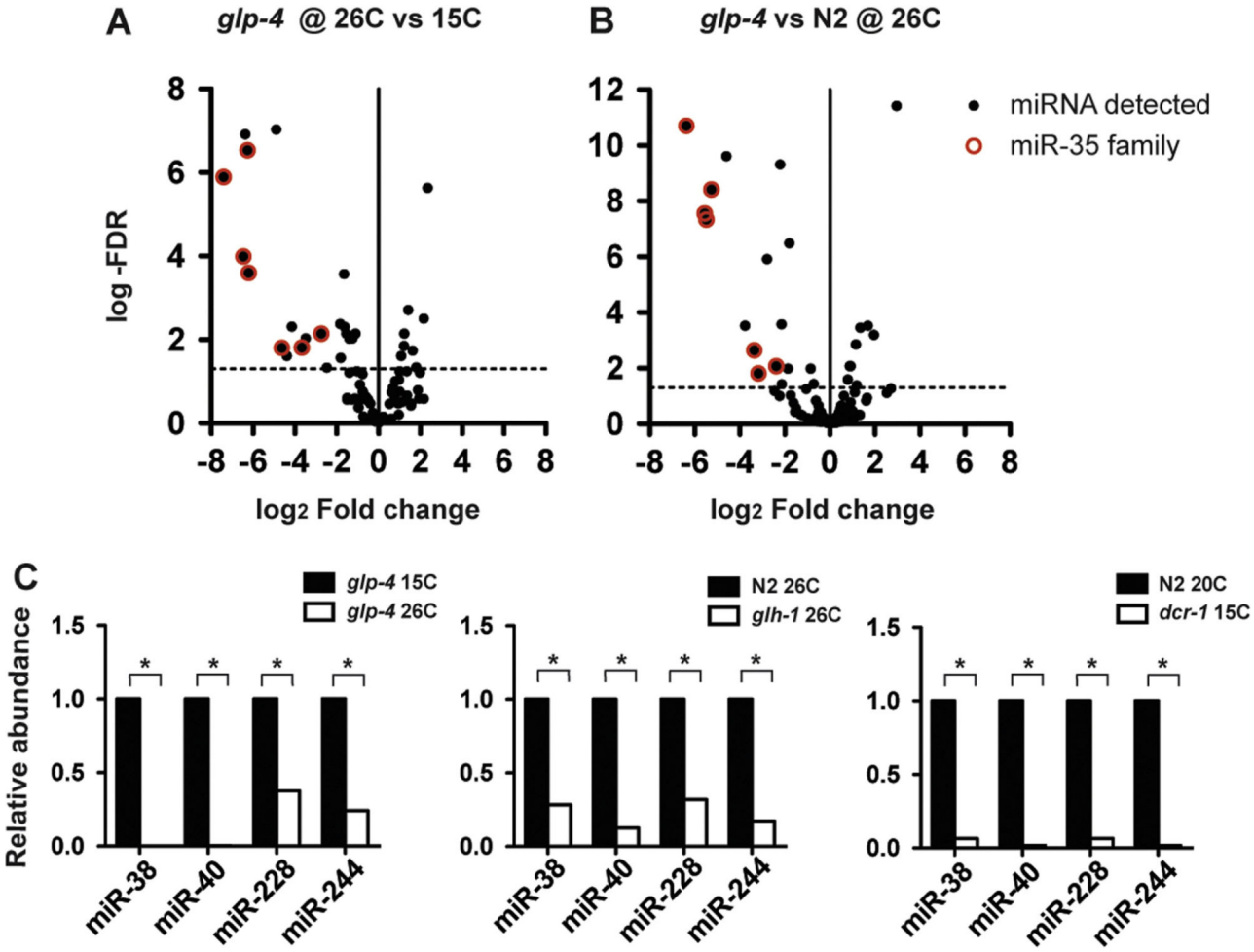

Fig. 1. Multiple miRNAs are affected by loss of the germline

A The miRNAs that significantly change when sterile *glp-4* worms grown at 26° are compared to fertile *glp-4* worms grown at the permissive temperature of 15° on this volcano plot produced with Prism software. All 93 miRNAs detected in our adult populations are plotted here (black dots). The 21 miRNAs that decrease when the germline is missing are in the left quadrant; seven members of the *miR-35* family are indicated in red. In addition, eight miRNAs, seen in the right quadrant, significantly increase in the *glp-4* miRNA population when the germline is missing. The 64 miRNAs that showed no change, or changes not meeting the criteria for significance, are clustered in the center of the A plot below the dotted horizontal cutoff line which indicates a FDR(False Discovery Rate), using the q-value of <0.05 for significance. The data plotted in figure is presented in Table 1A–C, for the significantly changing miRNAs and in Supplemental Table S3A–C for all 93 miRNAs detected. **B** This volcano plot, similar to that in 1A, compares abundance of *glp-4* 26° miRNAs with those of N2 worms grown at the same temperature. **C** qRT-PCR verifies the relative abundance of *miR-38, miR-40, miR-228* and *miR-244*. Levels of *miR-38,-40,-228* and *−244* were assayed using both biological and technical triplicates by qRT-PCR comparing small RNAs from *glp-4* 26° sterile worms to those of *glp-4* 15° fertile worms (panel 1); *glh-1* 26° sterile mutants compared to N2s at 26° (panel 2); and

homozygous, sterile *dcr-1* 15° animals vs. N2s at 20° (panel 3). U18 was used as the endogenous control for each condition and strain tested. The statistical significance of differences in relative levels of miRNAs was determined using the Relative Expression Software Tool (REST) 2009 (www.gene-quantification.de/rest.html). The brackets with an asterisk in C indicate the p-value is statistically significant (p-value <0.0001). Numerical results are given in Table 2.

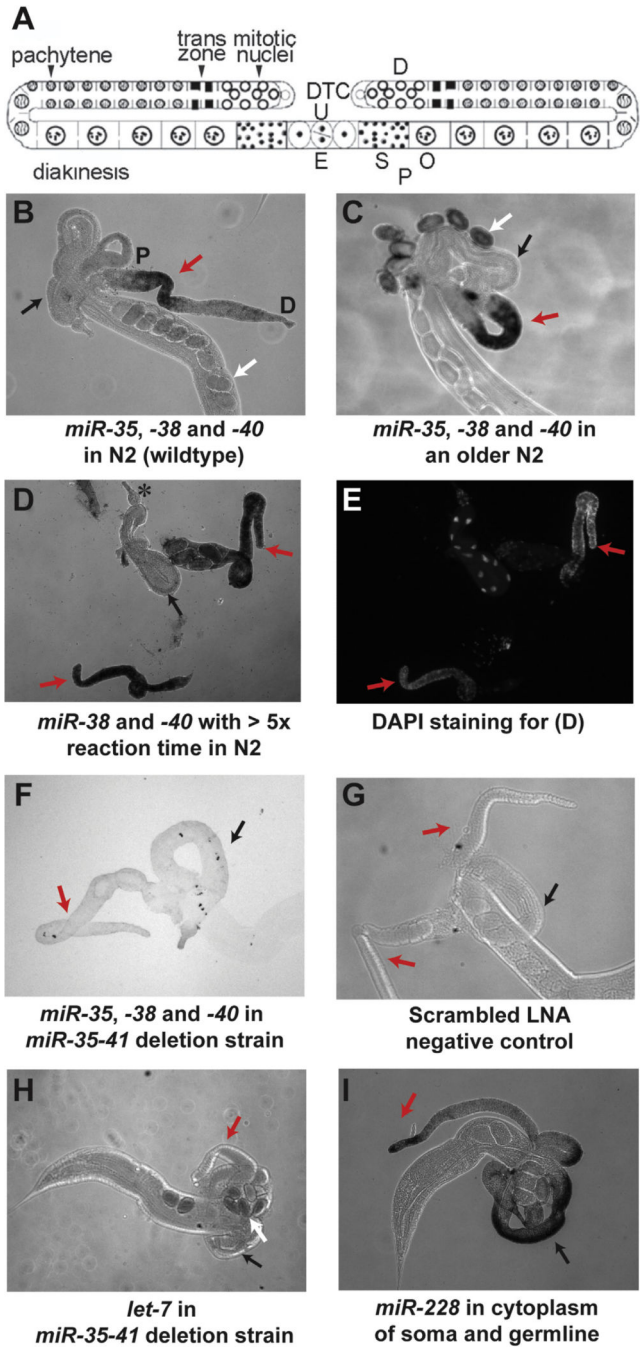

Fig. 2. *In situ* hybridizations indicate *miR35* miRNAs are exclusively detected in the adult germline, while *miR-228* is present in both germline and somatic tissue

A provides an illustration of the *C. elegans* adult bi-lobed gonad from (Smith et al., 2002) revealing the progression of germline development from the mitotic region in the distal gonad (D) beginning at the distal tip cell (DTC), with germ cells transitioning into meiosis (trans. zone) with oogenesis (pachytene and diakinesis) producing mature oocytes (O) in the proximal gonad (P) which contains mature sperm (S) in the spermatheca. After fertilization the embryos (E) develop and are later released, at about the 40-cell stage, through the vulva (V). In B-I and in Supplemental Fig. S3A several *C. elegans* miRNAs were localized by *in*

situ hybridization to adult worm tissues using LNA probes complementary to *miRs-35,−38* and *−40*, *miR-228*, a Scrambled LNA (a negative control), *let-7*, and to an LNA complementary to pre-SL-1 (a positive control). In each case, unless otherwise indicated, the total concentration of individual or combined probes did not exceed 25 nM and all worms were wild type (N2). All images were taken at the same 100X magnification.**B** is a whole hermaphrodite adult splayed open to expose the intestine and the germline. The worm was hybridized with a combination of *miR-35, −38,−40* probes, revealing a signal concentrated in the meiotic pachytene region (the area of bend in the gonad, red arrow), with no signal seen in the gut (black arrow). In all images in this figure and Supplemental Fig. S3C the germline is marked with red, somatic tissue with black, and embryos with white arrows. Unless otherwise indicated, worms were young adults 1–2 days beyond the L4 stage (>L4) and grown at 15°, because the lower growth temperature extends the lifespan and a “young” adult worm state (Kato et al., 2011). The color reactions were carried out in two steps for a total of ~60 min, unless otherwise indicated. **C** shows an older adult (2–3 days >L4) also hybridized with the three *miR-35* family LNAs and again the signal is concentrated in the mid-section of the germline tissue, in the meiotic, pachytene region (red arrow). In this image the combined *miR-35s* probe also hybridizes throughout all the cells in the extruded embryos (white arrows) of this older adult. **D** illustrates the use of two *miR35* family probes, *miR-38 and −40*, on the two gonad arms and an intestinal tract that were completely removed from a young N2 adult grown at 26°. Here the final color reaction was allowed to proceed for 5.5 h. It is clear that the positive signal remains concentrated in the germline, although it is now throughout the two separated arms of the bi-lobed gonad (red arrows) and remains absent from the somatic intestine (black arrow). An asterisk marks the extruded pharynx. This longer exposure reveals that *miR35* miRNAs, while abundant and concentrated at the pachytene stage of meiosis, are also present at lower levels throughout the germline, including the proliferative distal region (red arrows). **E** is the DAPI image of panel D. **F** shows a MT14119 *miR-35-41* worm raised at 15°, splayed and hybridized with the *miR-35, −38*, and *−40* combination. While this worm is negative, in some cases the deletion mutant shows weak hybridization, perhaps due the match of the LNAs to the “seed” sequence of *miR-42*, a family member not deleted in this strain. In **G** a Scrambled LNA, a second negative control, was used for the hybridization; this probe consistently produced no signal. **H** shows the *let-7* LNA on an MT14119 *miR-35-41* older adult grown at 26°. As with N2 adult worms (not shown), the *let-7* LNA does not hybridize to adult tissue. At this non-permissive temperature the *miR-35-41* deletion strain retains aberrantly developing embryos and it appears the *let-7* probe uniformly hybridizes throughout these embryos (white arrows). **I** shows an *in situ* hybridization of *miR-228* on an N2 worm grown at 26°. *miR-228* localizes in the adult germline, especially at the distal region of the gonad (red arrow) and is also detected in the somatic gut (black arrow).

Table 1

Statistical analyses of sterile germline-defective mutants compared to fertile worms

These tables show the miRNAs that significantly change in each comparison. A The DESeq2 analysis of *glp*-415° miRNAs compared to *glp-4* 26°. B DESeq2 calls of significance for *glp-4* 26° vs. N2 26° miRNAs. C The DESeq2 analysis for *glh-1* 26° vs. N2 26° miRNAs. To view the results of statistical analyses for all detectable miRNAs see Supplemental Table S3A–C.

	log2 fold change	Adj. P-value
A. *glp-4 (bn2) 26C vs 15C*		
miR-4813	−4.89605	9.30E−08
miR-260	−6.36403	1.21E−07
miR-39	−6.26213	2.89E−07
miR-38	−7.40438	1.29E−06
miR-248	2.35392	2.35E−06
miR-35	−6.45842	0.0001017
miR-37	−6.21010	0.000252791
miR-70	−1.64195	0.000267552
miR-238	1.41267	0.001948051
miR-239.1	2.16398	0.003155295
miR-2212	−1.83031	0.004223912
miR-262	−4.15019	0.004887495
miR-240	−1.62272	0.004995897
miR-2214	1.23544	0.00714549
miR-244	−1.09378	0.00714549
miR-42	−2.73965	0.00714549
miR-73	−1.53514	0.00714549
miR-1830	−3.47870	0.00930712
miR-56	−1.24676	0.00930712
miR-1022	−1.38437	0.009435131
miR-53	1.21911	0.014087703
miR-40	−3.66994	0.015520947
miR-36	−4.62137	0.015631642
miR-60	1.63146	0.018428118
miR-4931	−4.38697	0.024686066
miR-71	1.08388	0.024686066
miR-788	−1.80748	0.02719458
miR-4916	1.80619	0.045959487
miR-1832.1	−2.46817	0.046651332
B.*glp-4 (bn2) 26C vs N2 26C*		
miR-248	2.95717	3.85E−12
miR-38	−6.37337	1.95E−11
miR-4813	−4.59489	2.43E−10
miR-70	−2.20808	4.83E−10

	log2 fold change	Adj. P-value
miR-39	−5.25596	3.82E–09
miR-37	−5.55568	2.81E–08
miR-35	−5.48695	4.64E–08
miR-56	−1.79510	3.25E–07
miR-788	−2.79181	1.22E–06
miR-1829.3	−2.14947	0.00026497
miR-249	1.68721	0.00029823
miR-260	−3.76763	0.00029823
miR-71	1.35860	0.00035472
miR-239.1	1.96080	0.0006414
miR-238	1.15484	0.00139564
miR-40	−3.35445	0.00226176
miR-42	−2.38211	0.00835347
miR-53	0.88166	0.00835347
miR-58	0.92226	0.00835347
miR-244	−0.85106	0.01037996
miR-43	−1.86624	0.01037996
miR-36	−3.16671	0.01530756
miR-72	0.80125	0.02515828
miR-65	−0.70855	0.03634389
miR-61	−2.13195	0.03755028
miR-60	1.19401	0.04133958
C. ***glh-1 (gk100) 26C vs N2 26C***		
miR-244	−1.32081	1.44E–06
miR-4813	−2.32621	1.24E–05
miR-72	0.95901	0.00615274
miR-58	0.91224	0.01032463
miR-237	−0.91340	0.01035653
miR-56	−0.96261	0.0113635
miR-64	0.69839	0.0113635
miR-788	−1.56113	0.0113635
miR-51	1.08469	0.01302394
miR-85	0.68831	0.01302394

Table 2

Relative abundance of mature miRNAs in TaqMan® miRNA assays. qRT-PCR was utilized to assay *miR-38, miR-40, miR-228,* and *miR-244* levels in germline-minus *glp-4* 26° compared to fertile *glp-4* animals @15°, and in *glh-1* worms compared to N2s, both grown at 26°. Levels of these miRNAs were also measured in *dcr-1* null mutants, where they were expected to decrease. U18 was used as the endogenous control for each condition and strain tested. Statistical analysis with REST software (REST 2009) indicated that all three germline miRNAs tested were significantly decreased in comparisons at 26° of *glp-4* and *glh-1* worms, and in the 15° *dcr-1* mutant.

***glp-4 (bn2)*at 26C vs *glp-4* at 15C**				
miRNA	**Abundance**	**Std. Error**	**P-value**	**Result**
miR-38	0.001	0–0.006	< 0.0001	1000-fold down
miR-40	0.003	0.001–0.009	< 0.0001	333.3-fold down
miR-228	0.377	0.190–0.838	< 0.0001	2.7-fold down
miR-244	0.242	0.093–0.601	< 0.0001	4.1-fold down
***glh-1(gk100)* at 26C vs N2 at 26C**				
miRNA	**Abundance**	**Std. Error**	**P-value**	**Result**
miR-38	0.284	0.165–0.517	< 0.0001	3.5-fold down
miR-40	0.135	0.012–0.576	< 0.0001	8.0-fold down
miR-228	0.319	0.128–0.598	< 0.0001	3.1-fold down
miR-244	0.173	0.062–0.326	< 0.0001	5.8-fold down
***dcr-1(ok247)* at 15C vs N2C**				
miRNA	**Abundance**	**Std. Error**	**P-value**	**Result**
miR-38	0.065	0.045–0.114	< 0.0001	15.4-fold down
miR-40	0.018	0.010–0.027	< 0.0001	55.6-fold down
miR-228	0.066	0.043–0.106	< 0.0001	15.2-fold down
miR-244	0.017	0.007–0.042	< 0.0001	58.8-fold down